Microstructural characteristics, properties, synthesis and applications of mullite: a review

L. K. S. Lima[1], K. R. Silva[1], R. R. Menezes[1], L. N. L. Santana[1], H. L. Lira[1]
[1]*Federal University of Campina Grande, Academic Unit of Materials Engineering, 58429-900, Campina Grande, PB, Brazil*

Abstract

Mullite, an intermediate phase of the binary alumina-silica system, is one of the most important phases of ceramic products containing alumina and silica in the initial composition. Its stoichiometry ranges from $3Al_2O_3.2SiO_2$ (3:2) to $2Al_2O_3.SiO_2$ (2:1) and its crystalline structure is orthorhombic, characterized by the presence of octahedral chains of AlO_6 interconnected by tetrahedral chains of aluminum-oxygen and/or silicon-oxygen (AlO_4/SiO_4). Properties such as high chemical and thermal stability, low thermal expansion and conductivity, and good mechanical strength enable a wide range of applications. Due to the relevance of this material, it is important for the scientific community to understand its microstructural characteristics, properties, methods of synthesis, and various applications. Therefore, this article aimed to make a comprehensive review on the mullite to gather and present to the reader a series of relevant information that makes it possible to deepen the knowledge about mullite.
Keywords: mullite, aluminosilicate, ceramic materials.

INTRODUCTION

Mullite is the only stable intermediate phase in the Al_2O_3-SiO_2 system at atmospheric pressure [1]. Due to its formation conditions, such as high temperature and low pressure, mullite occurs very rarely in nature. However, despite the scarce occurrence as a natural mineral, it has become one of the most important phases in traditional and advanced ceramics [1-4]. The most used methods for mullite synthesis are: sintering by solid-state reactions, resulting in the formation of mullite with the 3:2 stoichiometry (~72 wt% of Al_2O_3); crystallization of fused aluminosilicates, obtaining mullite with the 2:1 stoichiometry (~78 wt% of Al_2O_3); and heat treatment of organic or inorganic precursors. The chemical composition of mullite strongly depends on the precursors and synthesis temperature, and its morphology can vary between equiaxial grains, flakes, and needles [2, 5, 6]. The great technical and scientific importance of mullite is due to factors such as: high chemical and thermal stability (melting point ~1830 ºC); low coefficient of thermal expansion (~4.5x10^{-6} K^{-1}) and thermal conductivity of ~6 kcal/(m.h.K); good mechanical strength (~200 MPa); availability of raw materials rich in Al_2O_3 and SiO_2; ability to form crystals from various proportions between Al_2O_3 and SiO_2; ability to incorporate a wide variety of cations in its structure; structural principles that can be extended to a large number of phases that belong to the 'family of mullite-type structures' [2, 5]. All these characteristics make mullite very convenient for structural and functional applications, such as refractory bricks, filtration, catalyst support, refractory insulation, electronic substrates, membranes, humidity sensors, etc. [7, 8]. It is of fundamental importance that the scientific community has a good understanding of this material so that it can be better used and applied. Therefore, the objective of this review is to gather relevant information about the origin and the microstructural and morphological characteristics of mullite, besides presenting its properties, synthesis methods, and several applications.

HISTORY

Mullite can be found as a natural mineral on the Isle of Mull, Scotland (for this reason the name 'mullite'). Its occurrence in nature is rare, however, it can be prepared using various chemical compounds or natural raw materials [9]. Several researchers were part of the discovery of the mineral called mullite [10]. Oschatz and Wächter [11] observed crystallization processes in the vitreous phase of porcelain and, later, found that it was an acicular silicate rich in Al_2O_3, identified as sillimanite, which has the chemical formula Al_2SiO_5. Deville and Caron [12] identified the existence of a compound with approximately 70.5 wt% of Al_2O_3 and associated it with sillimanite. Vernadsky [13] also observed crystalline phases similar to sillimanite in porcelain. More than a hundred years ago, geologists from the British Geological Survey explored the Isle of Mull, located on the west coast of Scotland, and collected mineral samples from places where lava flow from the Ben More volcano was common. The geologists found acicular minerals rich in Al_2O_3, integrated with feldspar crystals, and initially, they were also identified as sillimanite. However, in 1924, Bowen and Greig [14] stated that the aluminum silicate stable in the Al_2O_3-SiO_2 system would have a 3:2 stoichiometry ($3Al_2O_3.2SiO_2$), a phase resulting from the

*lizandralima15@gmail.com
https://orcid.org/0000-0002-8193-8652

contact between hot magma and clay sediments, instead of 1:1 stoichiometry ($Al_2O_3.SiO_2$) and proposed the name mullite to designate this compound. Rare occurrences of mullite have been found in SiO_2-rich glasses produced by the lightning impact on quartz sands, and also in small druses of volcanic rocks in the Eifel mountains, Germany [2, 15]. Since its discovery, a large number of studies have been carried out, which has influenced the use of mullite in several applications in the ceramic sector. According to Fig. 1, more than 8300 scientific papers directly related to mullite have been published, more than 6300 patents have been registered, and more than 79000 citations have been reported in the last 20 years, with an increasing trend [16].
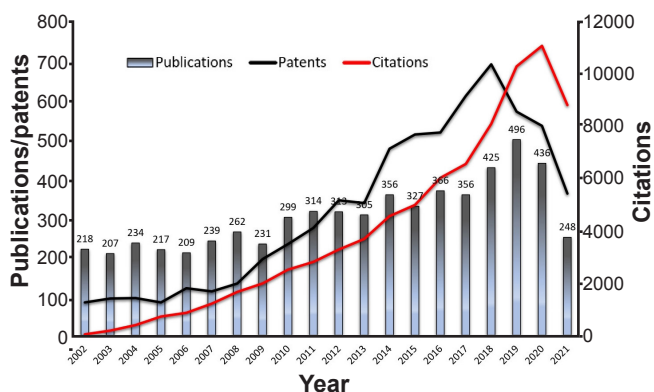

Figure 1: Number of scientific papers, patents, and citations directly related to mullite, since 2002 (data from [16]).

MICROSTRUCTURAL CHARACTERISTICS

Mullite 3:2 ($3Al_2O_3.2SiO_2$) is the only compound stable under atmospheric conditions of the Al_2O_3-SiO_2 system. It has an orthorhombic structure, characterized by the presence of octahedral chains of AlO_6 located at the vertices and in the center of the unit cell, with edges aligned in parallel along the 'c' crystallographic axis. The AlO_6 chains are interconnected by double tetrahedral chains of aluminum-oxygen and/or silicon-oxygen (AlO_4/SiO_4), also aligned in parallel with the c axis [15, 17-19]. Mullite has a crystalline structure closely related to that of sillimanite ($Al_2O_3.SiO_2$) and both have silicon and aluminum atoms located in tetrahedral sites. In sillimanite, the tetrahedral sequence of AlO_4/SiO_4 is regular and parallel to the c axis. However, in the mullite structure, there is no such regularity, since Si^{4+} cations can be replaced by Al^{3+} and the compensation of the charge deficiency induced by this substitution is achieved by removing an oxygen atom that joins a tetrahedral group. Thus, there is the formation of an oxygen vacancy ($\square$) that leads to a structural rearrangement, displacing the excess of Al atoms to a new position, and forming an oxygen-deficient tricluster, that is, three tetrahedra sharing the same oxygen atom [1, 2, 15, 20, 21]. The substitution reaction can be described according to Eq. A. Fig. 2 shows the changes in the sillimanite structure, when it is converted to mullite.

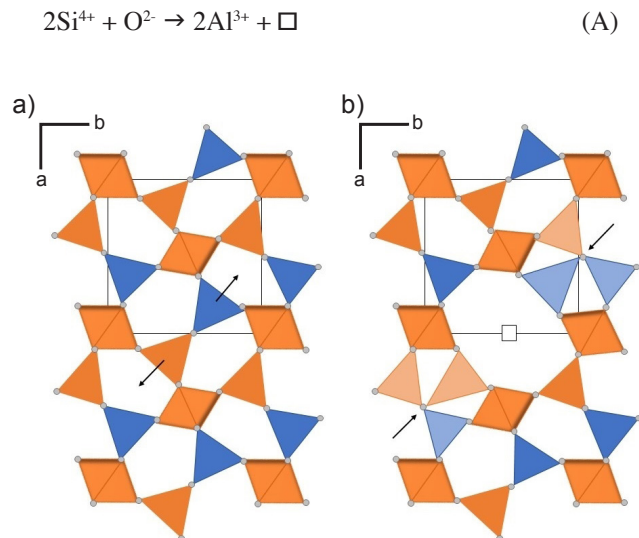$$2Si^{4+} + O^{2-} \rightarrow 2Al^{3+} + \square \tag{A}$$

Figure 2: Structure of sillimanite (a), being converted into mullite (b). The planar images represent a structure parallel to the 'c' axis. The arrows demonstrate the structural changes from sillimanite to mullite, where in (a) they are indicating the migration directions of the Al atoms that were linked to the oxygen that was removed, and in (b) they are pointing to the atoms making new bonds between tetrahedra. The square indicates the oxygen vacancy originated from the charge balancing reaction.

The crystalline structure of mullite 3:2 is orthorhombic. However, the structure can vary according to the formation temperature and alumina content since it changes the network parameters. When mullite is produced using mixed molecular precursors at temperatures below 1200 ºC, the first crystals tend to be rich in Al_2O_3 (approximately 80 mol%) regardless of the mass composition of the precursors. These crystals have a unit cell network parameter 'a' that is very close in size to the parameter 'b'. Therefore, this structure was called 'pseudotetragonal mullite', since crystalline symmetry is still orthorhombic even when the network parameters a and b are practically equal in length [20, 22]. On the other hand, when the content of Al_2O_3 is above 80 mol%, a>b and the crystalline structure is difficult to comprehend. Thus, the conventional mullite structure model is restricted to contents lower than 80 mol% of Al_2O_3, where all possible vacancies are formed. When the content of Al_2O_3 is greater than 80 mol%, some additional Al^{3+} ions are incorporated into the interstitial sites of the mullite structure and with the content of Al_2O_3 equal to 50 mol%, the sillimanite network parameters are identified [2, 15, 23].

Often, mullite comes in the form of a solid solution, which can be described by the chemical formula $Al_{(4+2x)}Si_{(2-2x)}O_{(10-x)}$. The x represents the number of oxygen vacancies present in the structure. It is a function of the content of silica and alumina, and changes from 0.20 to 0.90 (corresponding to approximately 55-90 mol% of Al_2O_3). For 3:2 mullite, x=0.25, and for 2:1 mullite, x=0.40 [1, 2, 22, 24, 25]. However, diffusion
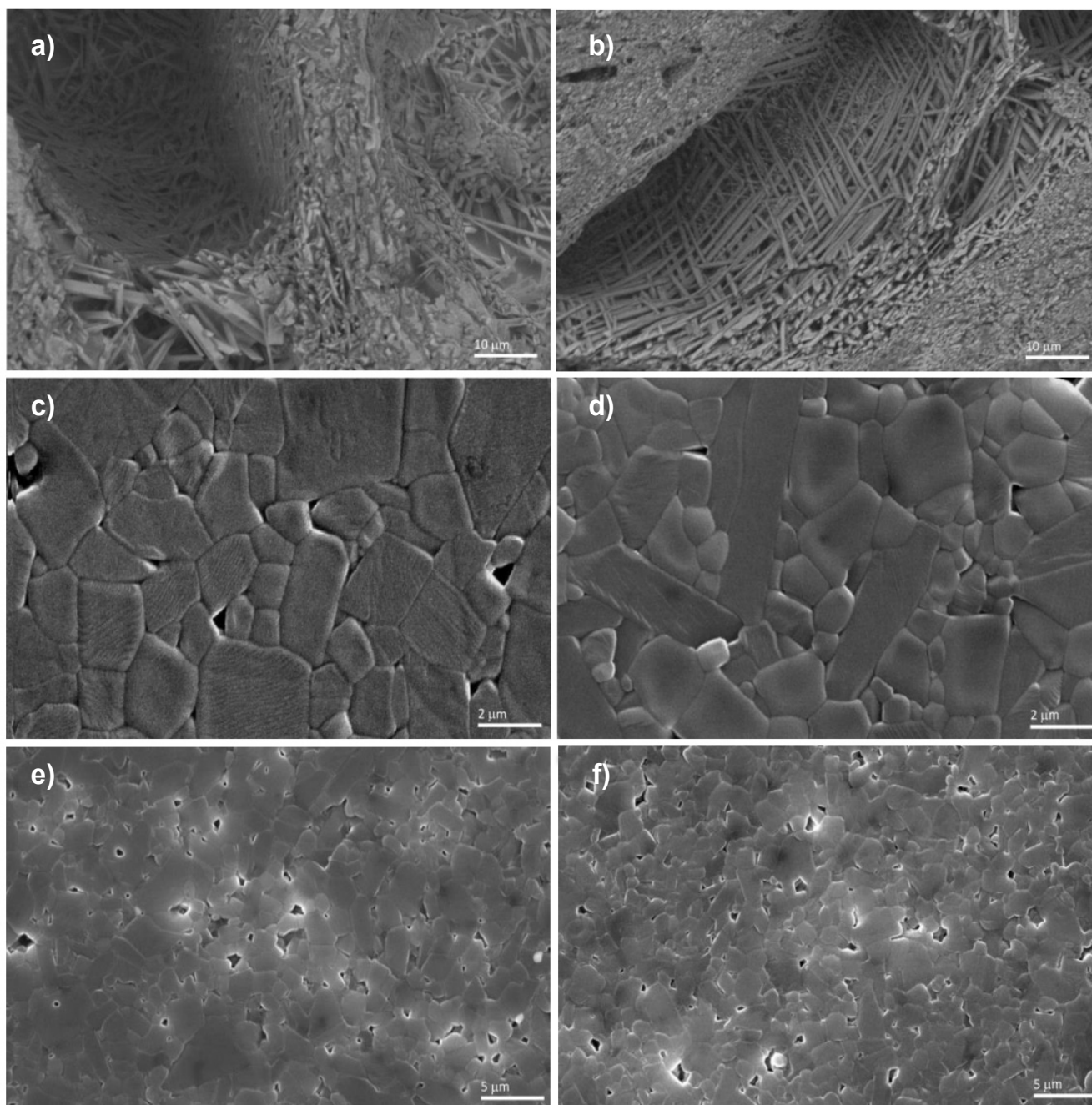
Figure 3: SEM micrographs showing: mullite crystals in porcelains sintered at 1350 °C (a,b); mullite samples (density 95%) sintered in microwave oven (1.5 kW, 16 min) (c) and conventional oven (high vacuum) at 1650 ºC/2 h (d) [29]; mullite samples sintered at 1600 °C with heating rates of 5 °C/min (density 90%) (e) and 80 °C/min (density 78%) (f) [30].

studies have shown that the chemical formula $Al^{VI}_{(4/3+14x/3)}(Al^{IV}_{8/3}Si_2)_{(1-x)}O_{(10-x)}Y_x$ is more appropriate, although it is not commonly seen in the literature [1, 26]. The Y corresponds to oxygen vacancies, the superscripts IV and VI indicate, respectively, tetrahedral and octahedral coordination. Depending on its chemical composition, mullite can be classified as primary and secondary. The primary mullite has an alumina:silica molar ratio of 2:1 ($2Al_2O_3.SiO_2$) and 3:2 ($3Al_2O_3.2SiO_2$) for the secondary mullite [22, 27, 28]. The compositional difference is also reflected in its microstructure, which varies from a platelet (ratio of 2:1) to a needle shape (ratio of 3:2) [22]. A factor that also influences mullite morphology is the type of synthesis. Monocrystals of mullite obtained by melting the raw materials are acicular or columnar and can reach several centimeters long, whereas mullite derived from the sol-gel process generally have extremely small crystallite sizes with nano dimensions. The mullite crystals produced by sintering reactions have dimensions that vary from 1 to 100 μm, with acicular or equiaxial morphology [15]. Fig. 3 shows micrographs of mullite crystals obtained through solid-state sintering reactions.

PHASE DIAGRAM

The first phase diagram for the Al_2O_3-SiO_2 system was published in 1909. Until then, it was believed that the only binary compound in this system was sillimanite (Al_2O_3.SiO_2). However, under standard conditions, this compound showed to be metastable. It was found that it reached stability only at high pressures [10]. In 1924, researchers verified that the stable aluminosilicate at standard conditions was the one with the composition $3Al_2O_3$.$2SiO_2$, which melted at approximately 1810 ℃ [14]. Mao et al. [31] mentioned some works that identified the melting point at 1933 and 1900 ℃. Mullite was initially considered as a stoichiometric compound, but with the development of many studies related to this material, it was discovered that it could have a considerable range of composition [31]. The solid solution range of mullite has been reported to extend from 71.8 to 74.3 wt% of Al_2O_3 under stable conditions. However, this range is valid only when mullite is prepared by solid-state reactions in the presence of alumina [32].

Studies carried out in the Al_2O_3-rich region, contained in the Al_2O_3-SiO_2 system phase diagram, showed a great disagreement in the literature about the type of fusion that occurs in mullite, which can be congruent or incongruent. There is accumulated evidence in favor of both processes. In this system, when the mullite melts congruently, a liquid phase with the mullite composition is obtained. On the other hand, the products of the incongruous fusion are corundum (Al_2O_3) and liquid, both with different compositions from mullite [33]. Bowen and Greig [14] noted that when natural rocks were immersed in hot magma, the products were invariably sillimanite and corundum. Based on this observation, the authors used natural sillimanite and artificial mixtures of Al_2O_3 and SiO_2 to prepare compositions that were heated at a high temperature for complete melting and then slowly cooled. For each composition, a good amount of corundum crystallized along with a liquid phase. Therefore, they concluded that the mullite melted incongruously. Bowen and Greig's studies lasted for several years without major objections, until other researchers began to study the synthesis of mullite crystals by the flame fusion method (Verneuil's method), achieving success in their experiments. Thus, they concluded that if mullite were an incongruous fusion compound, this method of synthesis would not have been possible. These contributions confirmed the hypothesis of congruent mullite fusion and, since then, this discussion in the literature has been intense [34, 35]. Aramaki and Roy [36] stated that, in studies related to phase diagrams, better results are obtained when sealed systems are used. Thus, the authors prepared different mixtures from α-alumina and glassy silica powder, which were subjected to high temperatures in sealed containers to prevent silica loss. After heating, the samples were directly cooled, in most cases, by placing them in a mercury container with a little water on top. Containers were opened and samples were examined under a polarizing microscope. They found a congruent melting point at approximately 1850 ℃, with the formation

of mullite on cooling, from the liquid that was completely homogeneous. For none of the mixtures, corundum was found after mullite melting. Mao et al. [31], Toporov and Galakhov [34], and Staronka et al. [35] also proved the mullite's congruent fusion in their works.

Klug et al. [37] reinvestigated the Al_2O_3-SiO_2 system phase diagram in the mullite region. The researchers prepared high-purity polycrystalline samples of various compositions and examined the phase changes that occurred during heating and cooling. According to the results, the mullite undergoes incongruous fusion at 1890 ℃. Gelsdorf et al. [38] observed this process at around 1820 °C. Skola [39], who collected specimens of mullite and also sillimanite blocks used in glass tank furnaces and metallurgical furnaces, showed by microscopy and X-ray diffraction that in all cases the mullite melted incongruously, obtaining corundum and a vitreous phase at the end of the process. Melting did not take place at such a high temperature, as noted by the aforementioned authors (1820-1890 ℃) and also Bowen and Greig [14] (1810 °C). However, the author reported that, in a longer dwell time, the temperature of 1450 °C was enough. Aksay and Pask [32] determined the mullite phase equilibrium above 1800 °C and therefore its melting behavior. For this purpose, the authors used a previously studied technique that involves the diffusion by semi-infinite pairs of SiO_2 and Al_2O_3 and an electron microprobe. They also encapsulated the samples to prevent silica loss. According to their studies, the most important feature of the diagram obtained from the diffusion studies is that, under stable equilibrium conditions, mullite melts incongruously at 1828 °C, as originally determined by Bowen and Greig [14]. In another study, Risbud and Pask [40] proposed a metastable phase diagram of the Al_2O_3-SiO_2 system, which was obtained after experiments using a mixture of Al_2O_3 and SiO_2 with the mullite stoichiometric proportion, heated to temperatures of approximately 2000 ℃ and, subsequently, cooled. The decrease in temperature reduces the saturation of Al^{3+} ions in the structure, leading to supersaturation of the silico-aluminous liquid, which, consequently, tends to remove excess ions by nucleating the α-alumina phase and, thus, restoring balance. A further decrease in temperature supersaturates the liquid again with Al^{3+} ions and induces the precipitation of α-alumina, leading to the growth of previously formed nuclei. In these early stages, there is no nucleation of the mullite because the temperature is still higher than the melting temperature of this phase. If the cooling rate is slow, the time that the liquid remains at temperatures above 1828 ℃ (melting of mullite) and below 2054 ℃ (melting of alumina) is sufficient to precipitate a large amount of α-alumina. In this way, when temperatures below 1828 ℃ are reached, the liquid is poor in Al^{3+} ions, making it difficult to form the mullite phase. On the other hand, if the cooling rate is high, the time in which the silico-aluminous liquid remains at temperatures above 1828 ℃ is too short to allow the nucleation of α-alumina and, consequently, only the mullite phase is formed. For moderate cooling rates, both phases are formed: mullite and α-alumina. In this case, the time above 1828 ℃ is sufficient

for the diffusion of a small amount of Al^{3+} ions and nucleation/precipitation of a reduced content of the α-alumina phase. Thus, when the liquid reaches temperatures below 1828 ºC, there are still enough Al^{3+} ions for the formation of mullite [40].

The composition of mullite obtained by reactions in a liquid state can extend up to 82.6 wt% of Al_2O_3 thus raising the question of the existence of a disordered form of mullite with the nominal composition of $2Al_2O_3.1SiO_2$ [32]. The experiments performed by Aksay and Pask [32] generated information about stable equilibria (slow heating and cooling) and several metastable phases (rapid heating and cooling). The authors stated that under metastable conditions, ordered mullite melts congruently at 1880 °C and its solid solution range extends up to 77 wt% of Al_2O_3. Under the same conditions, the disordered mullite melts congruently at a temperature of approximately 1900 °C. The existence of metastable systems is associated with the overheating of mullite above the incongruous melting temperature and the nucleation of alumina and mullite in supercooled aluminum silicate liquids [32]. Tromel et al. [41] used pure sources of SiO_2 and Al_2O_3 to study the Al_2O_3-SiO_2 system. The results of chemical analysis, X-ray diffraction, and microscopy of samples heated (1870 °C/5 min) and rapidly cooled revealed that the only phases present were mullite and a glassy phase. However, corundum and vitreous phase were found in the samples when a long period of heating (up to 1870 ºC/8 days) and cooling were applied. Therefore, it was established that the mullite showed both incongruent and congruent fusion depending on the heating and cooling conditions of the mixtures. A slow rate allowed the mullite to reach a stable equilibrium and caused incongruent fusion, but the metastable equilibrium persisted during a fast rate, which promoted a congruent fusion process.

Given the variety of results related to the type of mullite melting found in the literature, there is no basis for supposing that one concept is correct and another is incorrect. It is necessary to review the nature of each experiment, where the variation in results may depend on the raw materials and the experimental methods used. In addition, bonding forces, free energies, and crystalline structures can also influence the equilibrium [10]. In a careful analysis of the Al_2O_3-SiO_2 system phase equilibrium studies, it becomes possible to highlight some factors that can influence the mullite's melting behavior, such as: the loss of silica from the mixtures by evaporation, which could facilitate the corundum nucleation, without much change in bulk composition, leading many authors to regard mullite as an incongruous fusion compound [36]; impurities in the raw materials that may favor the production of mullite, but at high concentrations may favor the decomposition of the mullite releasing corundum, and leading to congruent fusion results to be interpreted as incongruent fusion; kiln atmosphere, since reducing and inert environments, or an atmosphere with low partial pressure of oxygen favor the decomposition of mullite into corundum; furthermore, free or combined silica in mullite can also be easily reduced by

these agents; the rate of heating and cooling; the existence of stable and metastable balances; the nucleation and growth of corundum crystals in mullite after fusion due to its ability to retain a large amount of Al_2O_3 in solid solution; as well as phase identification and study techniques can influence the interpretation of results related to this process [42].

PROPERTIES

The wide technical applicability of mullite ceramics is derived from its excellent properties, such as high thermal stability, excellent thermal shock resistance, low thermal expansion and conductivity, adequate mechanical strength, and creep resistance. Mullite ceramics also have low gas permeability and excellent deformation resistance, compressive strength, good corrosion resistance in severe environments, and good dielectric properties [2, 8, 15, 17, 18, 43-47]. The technically relevant properties of mullite ceramics are shown in Table I. The collected data demonstrate the high potential of mullite for numerous applications, in traditional and advanced ceramics.

Depending on the microstructural characteristics, the low fracture toughness of mullite (1.5-3 MPa.m$^{1/2}$), which does not change considerably with increasing temperature, can be considered a significant factor in limiting potential applications, but the other properties outweigh this disadvantage. This low tenacity must be taken into account according to the application for which a certain material is designed, as this parameter demonstrates the fragile character of mullite [21]. Mullite's slow diffusion kinetics provide excellent microstructural stability at high temperatures. In addition, mullite generally has a minimal amount of vitreous phase in the grain boundaries, due to the diffusivity rates

Table I - Technically relevant properties of mullite ceramics.

Composition	$3Al_2O_3.2SiO_2$ [2, 14]
Melting point (ºC)	1810-1890 [14, 36, 39, 40]
Coefficient of linear thermal expansion, 20-1400 ºC (10^{-6} K^{-1})	~4.5 [2, 15]
Thermal conductivity	
at 20 ºC (kcal.m^{-1}.h^{-1}.K^{-1})	~6 [15]
at 1400 ºC (kcal.m^{-1}.h^{-1}.K^{-1})	~3 [15]
Flexural strength (MPa)	~200-400 [2]
Fracture toughness (MPa.m$^{1/2}$)	1.5-3 [2, 21]
Electric conductivity	
at 550 ºC (Ω^{-1}.cm^{-1})	5.4x10^{-9} [15]
at 1400 ºC (Ω^{-1}.cm^{-1})	1.1x10^{-5} [15]
Refractive index	
n_α	1.630-1.670 [15]
n_β	1.636-1.675 [15]
n_γ	1.640-1.691 [15]

Note: unless otherwise stated, values are given at room temperature.

during sintering and also to its chemical composition, which consequently promotes good flexural strength (~200 to 400 MPa), which can vary in terms of density achieved, grain morphology, presence of additional crystalline and amorphous phases, and microstructure, especially porosity, which has a negative influence on flexural strength [21]. In polycrystalline mullites, generally, two behaviors can be observed. The first demonstrates a significant increase in flexural strength with increasing temperature. The second does not show a distinct maximum strength and this decreases slightly with increasing temperature. When mullite contains a small amount of vitreous phase at the grain boundaries, a noticeable increase in flexural strength occurs above the softening temperature of the vitreous inclusions, which may be associated with stress relaxation and/or crack healing. However, when the vitreous phase is crystallized to form cristobalite, this strength peak disappears [21].

Mah and Mazdiyasni [48] analyzed the mechanical properties from room temperature to 1500 °C of high purity (99.99%) and translucent mullite ceramics, prepared by hydrolytic decomposition of mixed metal alkoxides. The authors found that the mean values of four-point flexural strength were 128 MPa at room temperature, increasing to 140 and 145 MPa at 1400 and 1500 °C, respectively. These increases are explained by the presence of a small amount of vitreous phase which results in a strengthening of the mullite at high temperatures. Osendi and Baudin [49] studied the mechanical behavior of two mullite materials with the same level of impurities, but of different natures, at room temperature and up to 1400 °C. The results showed that the flexural strength values as a function of temperature showed similar trends for both mullite materials, with values of approximately 170 to 220 MPa at room temperature and showing strength peaks at 1200 and 1300 °C, ranging from 200 to 250 MPa. The authors reported that the increase in flexural strength at high temperatures can be associated with several phenomena derived from the softening of residual vitreous phases, which can lead to the weakening of critical failures. On the other hand, hot-pressed mullite ceramics with few impurities, a low amount of vitreous phase, and an equiaxed microstructure demonstrate a significant decrease in flexural strength at high temperatures. Kanzaki et al. [50] obtained a flexural strength value of ~400 MPa at room temperature and a slight decrease to 350 MPa when the temperature was 1300 °C. The authors reported that the decrease in flexural strength with increasing temperature was due to the overgrowth of grains and the absence of a significant vitreous phase occurring essentially at triple point junctions, but not at grain boundaries. Mizuno [51] reported flexural strength values at room temperature ranging from ~360 to 400 MPa. The strength measured at 1350 °C decreased to values of ~280-330 MPa and at 1400 °C they reached 270 MPa. Large grains increase in quantity and size, absorbing small grains with increasing temperature. Thus, it is believed that the change in specimen strength is also due to changes in

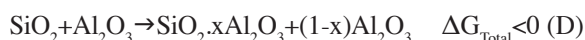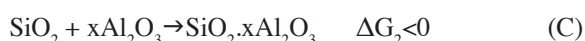microstructure, such as grain size and mullite grain size distribution.

The thermal conductivity of mullite ceramics is low, which makes this material an excellent thermal insulator. As the temperature increases, this property is exponentially reduced and, above 800 °C, it becomes almost constant. The temperature-induced development of the mullite's thermal conductivity can be explained by the phonon-phonon interactions, which at high temperatures become the main factor. However, at lower temperatures, the thermal energy in insulating materials is mainly transported by network vibrations [2]. Mullite is also an electrical insulator at room temperature, making it suitable, for example, as a substrate material for electronic devices. However, at high temperatures, based on electromagnetic field measurements, mullite ceramics exhibited high electrical conductivities [15]. According to Malki et al. [52], the evolution of electrical conductivity in mullite at high temperatures is characterized by two regions, which are at temperatures below and above 850-950 °C. At temperatures below 850-950 °C, electrical conductivity is considered low (~5.4×10^{-9} $\Omega^{-1}.cm^{-1}$ at 550 °C), while above, mullite exhibits higher electrical conductivity (~1.1×10^{-5} $\Omega^{-1}.cm^{-1}$ at 1400 °C). The authors explained the variation in the behavior of these materials as a function of the jumping of oxygen atoms connecting the tetrahedral double chains towards oxygen vacancies at high temperatures. These changes can contribute to an overall increase in conductivity. Due to this fact, the electrical conductivity of mullite is higher than that of α-alumina (without oxygen vacancies), but it is still much lower than that of doped zirconia (high concentration of vacancies).

Regarding optical properties, only some refractive indices (n) of mullite-type aluminosilicates are available, which have been shown to decrease linearly as the Al_2O_3 content increases. This decrease is reasonable since due to the increase in the number of oxygen vacancies, the density also decreases linearly [15]. Mullite ceramics have different refractive indices for different light propagation directions. The reported refractive indices of these materials range from 1.630 to 1.691 (Table I). While the birefringence ranges from 0.010 to 0.029, the 2 V optical axis angle ranges from 45° to 61°. Furthermore, some optical data prove the color variation that pure mullite ceramics and doped with different types of ions can obtain. For pure mullite doped with Ti^{4+}, colorless materials are observed, however, for mullite doped with Cr^{3+} and Fe^{3+} the colors observed are green and reddish-brown, respectively. In Eu^{2+}-doped mullite ceramics, the material exhibits strong blue-green emissions. Mullite nanoparticles doped with 8% Tb^{3+} and 0.1% Ce^{3+} are characterized by a strong green luminescence and these can be used in fluorescent lamps and display devices. Regarding optical transmittance, high transmittance data (>90%) were reported for wavelengths up to 5 μm, based on homogeneous, dense (porosity <1%) isostatically pressed mullite ceramics. The optical transparency or translucency of the mullite makes this material especially suitable for high-temperature oven windows [15].

SYNTHESIS

As a result of its mineralogical rarity, natural mullite deposits are unable to meet the growing demand for this material. In this way, its synthesis becomes increasingly important [53]. Mullite can be obtained through heat treatments or by chemical means, and the raw materials for its synthesis include alumina and silica, aluminosilicates such as sillimanite, kyanite [54-56], and andalusite [57-59], bauxite, laminated silicates rich in Al_2O_3, and clays. Kaolinite and other clay minerals have been widely used as raw materials since they allow various component shaping procedures, have low cost, are abundant in nature, and result in a simple method of producing mullite [2, 8, 60-62]. The raw materials, regardless of their method of preparation, may follow two routes of mullitization: the direct formation of mullite at temperatures of approximately 900 and 1000 ºC, which occurs when Al_2O_3 and SiO_2 are mixed at the molecular level, and the formation of mullite above 1200 ºC, when Al_2O_3 and SiO_2 are mixed in the level of particles [28, 62]. In addition, the development of mullite depends on the type of precursor, the particle size, the method of combining the reagents, and the heat treatment. In terms of composition, one of the most important factors to obtain this crystalline phase is the adequate amount of alumina and silica, with the stoichiometric proportion corresponding to 71.8 wt% of Al_2O_3 and 28.2 wt% of SiO_2, approximately [63, 64].

The formation of the mullite phase can be described by the following stage 1 (Eq. B) and stage 2 (Eq. C), and the total reaction (Eq. D) [60]:

$$\alpha\text{-}Al_2O_3 \rightarrow xAl_2O_3 + (1-x)Al_2O_3 \quad \Delta G_1 > 0 \qquad (B)$$

$$SiO_2 + xAl_2O_3 \rightarrow SiO_2.xAl_2O_3 \quad \Delta G_2 < 0 \qquad (C)$$

$$SiO_2 + Al_2O_3 \rightarrow SiO_2.xAl_2O_3 + (1-x)Al_2O_3 \quad \Delta G_{Total} < 0 \ (D)$$

Stage 1 corresponds to the dissolution of α-Al_2O_3. In this stage, there is the diffusion of Al^{3+} ions from the crystalline structure of the solid by breaking the alumina bonds. This event is energetically unfavorable since the rupture of the Al-O-Al connections raises the free energy of the system, that is, $\Delta G_1 > 0$. However, it occurs because of $\Delta G_{Total} < 0$ [60]. Stage 2 corresponds to the formation of the silico-aluminous liquid. During this stage, the silica structure is modified by the ions from the alumina, becoming a liquid of $SiO_2.xAl_2O_3$ composition. The x represents the number of ions from the alumina that diffuse into the silica structure and is related to the degree of saturation. This event is energetically favorable, since the Si-O-Al bond, predominant in the silico-aluminous liquid, has a lower energy state than the Si-O-Si and Al-O-Al bonds present in the silica and alumina solids, respectively. Therefore, $\Delta G_2 < 0$ [60]. The total reaction only occurs if the module of ΔG_2 (energetically favorable event) is higher than the module of ΔG_1 (energetically unfavorable event) so that ΔG_{Total} presents a negative value. This means

that the decrease in free energy caused by the formation of Si-O-Al bonds in the liquid must be greater than the energy increase caused by the dissolution of α-Al_2O_3. If $\Delta G_1 = \Delta G_2$, then ΔG_{Total} is zero, which means that the $SiO_2.xAl_2O_3$ formation reaches the equilibrium and for its continuation, it is necessary to increase the temperature, because, according to the thermodynamic equation $\Delta G = \Delta H - T.\Delta S$, raising the temperature (T) decreases the ΔG_{Total} of the system. This occurs due to the increase in the degree of saturation of Al^{3+} ions in the liquid, allowing higher values of x in the compound. Thus, more ions from the alumina can be incorporated into the liquid until the saturation of the system is reached again and a new balance is established. Each rise in temperature leads to an increase in the degree of saturation. When the degree of liquid saturation reaches a value where the amounts of ions Al^{3+} and Si^{4+} are close to the stoichiometric proportion of the mullite, the phase nucleation occurs. Thus, there is a temperature in which the value of x is equivalent to the composition of the mullite, and it is at this temperature that the mullitization of the system occurs with greater intensity [36, 60].

Based on the mullite formation mechanism, it is possible to reduce the temperature at which the reaction starts in three different ways, since this reduction is considered economically viable and of great interest on the part of the industry. They are [60]: i) use of more reactive raw materials: the presence of more reactive alumina contributes to the dissolution stage (stage 1), not requiring temperatures so high for sufficient quantities of Al^{3+} ions diffuse through the silico-aluminous liquid; ii) use of silico-aluminous sources that have Al^{3+} and Si^{4+} ions in contact at the molecular level: raw materials where the species involved (Al, Si, and O) are in close contact make the alumina dissolution stage (stage 1) unnecessary; in addition, only a short-range diffusion is needed, facilitating the formation of the $SiO_2.xAl_2O_3$ compound (step 2); and iii) addition of phase mineralizing agents: as soon as the Al^{3+} ions are dissolved in the silico-aluminous liquid, they can precipitate in the previously formed mullite nuclei, without the need for the liquid to be saturated by these ions, allowing the mullite grains to grow at low temperatures.

Synthesis by reactive sintering

The synthesis of mullite by reactive sintering consists of two processes: solid-state synthesis which refers to mullite synthesized after heating to a temperature below its melting point, with crystallization and densification of the phase; and liquid state synthesis, where mullite is obtained by heating the mixtures of alumina and silica to a temperature above their melting point, followed by cooling to crystallize the phase [10].

Solid-state synthesis: in this method, mullite can be produced by means of solid-state diffusion reactions of the raw materials, promoted by heating, resulting in micrometric-sized grains. During heating, the interdiffusion of ions begins at the interfaces between the particles of alumina

and silica. The ions from alumina diffuse, mostly, into the silica particles forming a silico-aluminous liquid. The diffusion of the ions continues with increasing temperature and the liquid gradually becomes richer in aluminum ions until the quantities of silicon and aluminum ions reach the stoichiometric proportion of the phase. Thus, the nucleation of mullite begins, followed by its growth, which occurs through diffusion and precipitation [60, 61, 65]. The mullite obtained by solid-state synthesis may be prepared from sillimanite group minerals, natural aluminosilicate minerals, such as kaolinite and topaz, and many types of oxides, hydroxides, inorganic and organic metal salts as precursors of alumina and silica. In these materials, oxides are atomically dispersed and Al-O-Si connections are frequent [60]. The minerals of the sillimanite group are transformed into mullite and silica when heated at high temperatures under oxidizing conditions. The topaz mineral, when subjected to heat treatment above 1400 °C, becomes acicular mullite and silica. The first researches related to the synthesis of mullite from pure oxides (Al_2O_3 and SiO_2) were driven by the work of Bowen and Greig [14], whose reactive mixtures were composed of purified precipitated α-alumina and quartz. In the work, the authors homogenized the raw materials in the desired proportion and heated them to a temperature close to 1700 °C. Then, the mixture was ground and reheated in the oven. This process was carried out five times and the formation of the mullite phase was studied. Since then, several studies have been carried out with many combinations of silica sources (quartz, cristobalite, silicic acid, fumed silica, fused silica) and alumina sources {α-alumina, γ-alumina, diaspore [α-AlO(OH)], gibbsite [$Al(OH)_3$], boehmite [γ-AlO(OH)]} [10].

Kong et al. [66] produced mullite from silica, alumina, and pentavalent oxides (V_2O_5, Nb_2O_5, and Ta_2O_5). The oxides were mixed using a conventional ball milling process and then specimens were shaped by uniaxial pressing and fired at temperatures between 1100 and 1500 °C. The authors observed mullite in mixtures that contained vanadium oxide and found that this oxide accelerated the formation of the phase. They also found that niobium and tantalum oxides inhibited mullitization. Aripin et al. [67] produced highly developed mullite from reactions between mixtures of α-Al_2O_3 powders and crushed silica from sago ash. The analyzes were performed on cylindrical samples sintered at temperatures ranging from 900 to 1700 °C. The authors found that with the increase in the content of α-Al_2O_3 in the initial composition of the samples sintered in the range of 1100 to 1700 °C, the amount of amorphous phase present in the structure decreased and the microstructure of the mullite became thick. Another important observation is that the first mullite grains were formed at a temperature of 1100 °C, which is a relatively low temperature. Chen et al. [68] produced transparent mullite ceramics from high purity α-alumina powders and amorphous silica (molar ratio of 63:37) at 1400 °C. The authors concluded that the method used in this work was promising for the preparation of transparent mullite ceramics. In kaolin, the mullitization occurs at lower temperatures than in pure oxides (approximately 1000 °C) and leads to the formation of acicular grains due to the presence of dissolved impurities, which induce the growth of these grains in preferential planes [60].

The weight ratio between silica and alumina in kaolin varies, with an excess of silica in relation to the stoichiometric proportion of mullite. Therefore, the use of kaolin together with other precursors rich in Al_2O_3 is a good alternative for obtaining mullite [18, 60]. Zhou et al. [69] produced porous mullite ceramics from kaolin and industrial alumina. They observed that the increase in temperature from approximately 450 to 600 °C led to the dehydroxylation of the kaolinite and partial breaking of the crystalline network, forming a disordered phase called metakaolinite. When 800 °C is reached, the first grains of primary mullite are formed. Then, at 960 °C, a liquid phase with a high SiO_2 content is formed, favored by the presence of kaolin impurities. During this process, Al^{3+} ions react in greater proportions with Si^{4+} ions from the silica-rich amorphous phase, forming the secondary mullite with needle-like morphology. As the sintering advances, the secondary mullite grows and, in the end, a porous structure is obtained with the presence of mullite with needle morphology and corundum and quartz particles. The temperature at which the ionic diffusion phenomenon occurs is considerably influenced by the particle size of the precursors. According to Kleebe et al. [70] and Gonçalves et al. [71], alumina particles with a greater specific area favored the dissolution of Al^{3+} ions in the siliceous glass phase, contributing to the nucleation and growth of mullite needles.

In situ production of mullite: several authors have proposed the use of *in situ* solid-state reactions to produce mullite based porous materials, including: highly porous castable structures for high-temperature applications [72], self-reinforced porous mullite ceramics [73, 74], ceramic foams reinforced by mullite whiskers [75], porous fibrous mullite bodies [76], porous mullite supports for membranes [77, 78], and cordierite-mullite nano-macro composites [79]. This synthesis technique, which produces monolithic mullite parts, represents significant energy and time savings, as well as offering advantages in comparison to other processes [72, 80, 81]. It consists of mixing 71-76 wt% of Al_2O_3 and 29-24 wt% of SiO_2 particulate sources, according to the Al_2O_3-SiO_2 phase diagram [32, 37, 72, 82, 83], shaping the specimens, and finally submitting them to a heat treatment. Many simultaneous reactions take place when the temperature is raised to 1200-1300 °C. The solid-state inter-diffusion process occurs at the contact points between Al_2O_3 and SiO_2 particles [72, 82, 84-86]. After a certain degree of diffusion of Al^{3+}, Si^{4+}, and O^{2-} ions, the crystal structure of the particles is locally destroyed, generating a metastable liquid with eutectic composition usually containing low melting point impurities [72, 87-89]. The formation of this liquid contributes to the dissolution of Al_2O_3, causing it to become an alumina-rich phase and, consequently, precipitating mullite crystals [72].

Intermediate reactions that take place during the

first stages of heating can affect the formation of mullite, depending on the raw materials used [72]. For example, the decomposition of some Al_2O_3 sources [$Al(OH)_3$, boehmite and kaolinite] at 200-450 °C [90-92] and quartz allotropic change at 520 °C [86, 93] produce pores and cracks in the structure, increasing the average interparticle space. The crystallization of amorphous silica in the tridymite and cristobalite phases at 800-1000 °C tends to decrease the interdiffusion rate of Al^{3+}, Si^{4+}, and O^{2-} ions, requiring higher temperatures and longer periods to complete the reaction [86]. On the other hand, raw materials containing fluxing oxides contribute to a greater diffusion of the aforementioned ions [84, 94]. Conventional SiO_2 sources for *in situ* mullite production include micronized quartz sand and fused silica, silica fume, and microsilica [72]. However, studies demonstrate the feasibility of using alternative sources, like fly ash [73, 78], waste silica fume [79], and rice husk ash [95]. On the other hand, conventional Al_2O_3 sources include calcined alumina, bauxite, boehmite, kaolinite, and $Al(OH)_3$ [72].

Liquid state synthesis: this synthesis allows to obtain high purity and high-density mullite. The process consists of melting the raw materials that are sources of Al_2O_3 and SiO_2 and subsequently cooling them, obtaining the crystallization of mullite. The raw materials that can be used in this method consist of sillimanite, alumina from the Bayer process, quartz sands, and fused silica, where the level of impurities is relatively low. The composition of crystallized mullite from liquids is, firstly, a function of firing temperature and, secondly, of the initial composition. The microstructure depends on the cooling rate and the Al_2O_3/SiO_2 weight ratio. Acicular mullite grains are obtained for the ratio value between 2.2 and 2.7, below 2.2 there is no mullite formation, and above 2.7 there is the formation of round grains. For the Al_2O_3/SiO_2 weight ratio greater than 3.3, the precipitation of α-Al_2O_3 occurs with mullite [21, 60].

Srivastava et al. [96] produced mullite particles through liquid state synthesis using sillimanite and alumina as raw materials and a thermal plasma reactor. The particles were used as reinforcement in a nickel matrix by the electrodeposition method to obtain Ni-mullite composite coatings. The Ni-mullite composite showed greater thermal stability and better wear and corrosion resistance compared to the reference composite (Ni-SiC). Therefore, they concluded that the mullite production method was effective. Kumar et al. [97] produced mullite through liquid state synthesis to use it as an abrasive in hybrid brake pads used to replace sintered bronze brake pads. This method of synthesis was used due to the high Mohs hardness of the mullite obtained through this process. According to the researchers, mullite was obtained effectively by the method and the results showed that the composition containing 3 wt% of mullite generated low-density pads with less vibrations and, consequently, the wear has been reduced. Therefore, the hybrid developed with mullite can be used to replace the conventional bronze brake pad for the desired application.

Mullite obtained by chemical methods

All chemical methods to obtain mullite basically consist of placing Al^{3+} and Si^{4+} ions in close contact [60]. The main methods used include: sol-gel [53, 98], precipitation [99, 100], and hydrolysis [60].

Sol-gel: this method is related to any process that involves a solution or molecules in suspension (sol) that undergoes a transition in which the solution or sol turns into a gel, establishing chemical bonds between particles or between molecular species, leading to the formation of a solid three-dimensional network. This method allows obtaining compositions with high chemical purity and homogeneity at the molecular level [53, 101]. A sol-gel process for obtaining the mullite phase consists of a mixture of colloidal particles of alumina and silica aiming the contact of the species at the nanometric level. Colloidal particles or molecules in suspension (sol) are subject to a chemical change that causes them to unite in a continuous network, forming the gel that is homogeneous and reactive [21, 60]. Different sources of silicon and aluminum precursors have been used for the synthesis of colloidal particles or mullite. In general, the precursor is an inorganic metallic salt (acetate, chloride, nitrate, sulfate, etc.) or an organic compound such as a metal alkoxide. The most used alkoxides are tetraethyl orthosilicate (TEOS) and tetramethyl orthosilicate (TMOS). In addition, another source of silica that has been used for the synthesis of mullite precursors is silicic acid, or an aqueous silica suspension. This route allows lower costs compared to the one that uses TEOS as a source of silica, however, it is not yet the most used [98].

In many cases, the reaction by the sol-gel method is essentially the same as for solid particles. However, the particle size differs significantly for the two preparation methods. The particle size of the sol is in the nanometer (nm) range and is, therefore, much smaller than those used in the solid-state reaction method, which is in microns (μm). In this way, a colloidal mixture can facilitate the reaction by several factors: first, nanometric compounds are more reactive, facilitating the dissolution of the alumina particles, since the increase in the surface area accelerates the reaction; another relevant factor is that the stoichiometric amount of Al^{3+} and Si^{4+} in small grains can be achieved by dissolving smaller amounts of alumina; and the third aspect is that in small particles, ions do not need to diffuse great distances [21]. Thus, when obtaining the agglomerates and submitting them to heating, mullite is obtained at lower temperatures than those commonly used in mechanical powder mixing processes [60].

According to Braga et al. [53], the gels obtained by the sol-gel method can be divided into two types, single-phase and diphasic, depending on the choice of reagents and the conditions of synthesis. Single-phase gels are produced when aluminum and silicon are mixed at the atomic level. These gels are formed from the replacement of silicon, in the three-dimensional network of silica, by atoms and/or hydrolyzed aluminum molecules, giving rise to Al-O-Si bonds similar

to those formed during the mullite crystallization stage [53, 102, 103]. In single-phase gels, crystallization of mullite occurs at a temperature of approximately 980 °C, without the formation of intermediate phases [33, 41, 66]. A mixture of silica and alumina at the atomic scale can be caused by the slow hydrolysis of a mixture of alkoxides and saline solutions. The crystallization process of mullite is controlled by the nucleation step, since the speed of this process depends on the presence of nucleating agents. For this type of gel, the activation energy for mullite crystallization is of the order of 400 kJ/mol [53, 102]. Diphasic gels are formed when the homogeneity scale is between 1 and 100 nm. In this case, there is usually the formation of transient phases prior to mullite crystallization, which generally occurs at temperatures close to 1300 °C. Diphasic gels can be formed through rapid hydrolysis of alkoxide or saline solutions. For this type of gel, the activation energy for the crystallization of mullite is in the order of 1000 kJ/mol [53, 102].

The reaction mechanisms for the mullite formation may vary considerably according to the precursors and the methods employed. Chemically synthesized precursors are converted into mullite in a temperature range between 850 and 1350 °C, and its chemical homogeneity scale determines the mullite formation mechanism and, consequently, its crystallization temperature. When the precursor has a high degree of homogeneity, the temperature at which mullite formation begins is low, however, when there is heterogeneity or segregation, even using chemical precursors, the mullite formation temperature is considerably increased, reaching temperatures above 1400 °C [53]. Rezaie et al. [104] compared mullite obtained from kaolinite, kaolinite with Al_2O_3, and boehmite with colloidal silica. Thus, they found that, between the three methods used, the colloidal compound was the one that generated mullite at a lower temperature (~1300 ºC). However, the grains were small and rounded. Tan et al. [17] prepared mullite fibers by the sol-gel process using aluminum carboxylates (ACs) and silica sol. The ACs were synthesized from the dissolution of the aluminum powder in a mixture of formic acid and oxalic acid using aluminum chloride hexahydrate as a catalyst. The gel fibers were completely transformed into mullite at 1200 ºC, with a smooth surface, dense microstructure, and uniform diameter. The activation energy for the formation of mullite fibers was 741.4 kJ/mol, which was less than most of the data reported in the literature. Zhang and Han [19] produced high purity mullite powders using the sol-gel method, with tetraethyl orthosilicate and aluminum nitrate as the main raw materials. The authors studied the properties of mullite powder under different pH values and other experimental conditions. In the gel preparation process, the temperature and heating time of the water bath were controlled, which contributed to forming a transparent and uniform gel. The results showed that the mullite was nucleated after 1000 ºC and crystals well developed with a low level of impurity were obtained at 1250 ºC. In addition, the increase in the calcination temperature was favorable for the refining of mullite grains, which presented a minimum size of approximately 50 nm.

In this context, there is also the hydrolysis method, which consists of preparing hydroxides in solution using a combination of silicon alkoxides and aluminum salts or mixtures of aluminum and silicon alkoxides. Hydrolysis occurs by adding water and sometimes acid or base is added as a catalyst [21]. The hydroxides formed are co-polymerized generating chains with the Si-O-Al structure. After polymerization, a solid is obtained that undergoes mullitization at low temperatures [71]. There are several limitations of this method. The most important of them is the fact that $Si(OH)_4$ and $Al(OH)_3$ polymerize at different rates, which makes it difficult to obtain the copolymer. It is important to note that the polymerization of $Si(OH)_4$ generates SiO_4^{4-} (mechanism of growth of colloidal particles and generation of the branched structure during the gelation of colloidal silica) and prevents mullitization, since the monomeric structure shares only the corners with AlO_4^{5-}, making interdiffusion and mullitization difficult [102].

Precipitation: this method consists of preparing mullite precipitates from a solution containing dissolved Al^{3+} and Si^{4+} ions (usually in organic solvent) using a precipitating agent [60]. There are two types of precipitation methods: co-precipitation and homogeneous precipitation. The first consists of the addition of a precipitant to a solution to form mullite precipitates. The second type consists of the previous dissolution of a precipitant in the solution and, subsequently, its pH change, causing the precipitant decomposition and, consequently, the precipitate formation [21]. In the mullite production process, precipitation is considered to have started when the formation of nuclei of the aluminum component with the silicon component is observed. In the case of co-precipitation, for example, this happens when the pH of the solution changes from acid to neutral due to the addition of an ammonia solution. The reason for this is that the solubility of the aluminum ion decreases rapidly between different pH conditions, while that of the silicon ion does not. The particles obtained are very small, but there is heterogeneity in the chemical composition due to the co-precipitation mechanism. The inner part of a precipitate is considered to have a composition rich in alumina, while the parts of the surface are rich in silica [21]. The main aluminum precursors for the process are nitrides, sulfates, chlorides, and aluminum alkoxides. On the other hand, the choice of precursors for the silicon component is restricted. Silicon alkoxides are commonly used and there have been only a few reports of the use of sodium silicate, silicon chloride, and silicon acetate. Ammonia and urea are generally used as precipitating agents [60].

APPLICATIONS

The combination of the properties of mullite makes it a ceramic material of great technological importance, with wide applicability, both in traditional and advanced ceramics. Among the various products in which mullite is present, the following stand out: refractories [105-110], porcelain tiles

Table II - Studies carried out with the objective of producing mullite for different applications.

Application	Raw material	Firing temperature	Synthesis method	Ref.
Refractory	Tabular alumina, reactive alumina, silica, mullite	1350-1650 ℃	Solid-state reactive sintering	[110]
	Industrial residues rich in aluminosilicates, bauxite	1500 ℃	Solid-state reactive sintering	[105]
	Kaolinite clay, quartz	>1200 ℃	Solid-state reactive sintering	[106]
	High alumina fly ash	1100-1400 ℃	Solid-state reactive sintering	[107]
	Fly ash from coal, different sources of alumina [$Al(OH)_3$, Al_2O_3, boehmite]	1025-1200 ℃	Solid-state reactive sintering	[108]
Porous ceramic	Fly ash from coal, alumina, starch, polyurethane sponges	1600 ℃	Solid-state reactive sintering	[115]
	Mullite powder, Isobam 104, sodium carboxymethyl cellulose, triethanolamine lauryl sulfate	1100-1250 ℃	Gelcasting and microwave sintering	[116]
	Coal fly ash, bauxite, V_2O_5, SiC, potassium feldspar	1450-1550 ℃	Solid-state reactive sintering	[117]
Ceramic membrane	Clay, $AlF_3.3H_2O$, alumina	1300-1500 ℃	Solid-state reactive sintering	[18]
	Coal fly ash, $Al(OH)_3$, MoO_3	1100-1500 ℃	Solid-state reactive sintering	[120]
	Coal gangue, $Al(OH)_3$, $(NH_4)_6Mo_7O_{24}.4H_2O$	1300-1450 ℃	Solid-state reactive sintering	[121]
Optical component	Mullite powder, α-Al_2O_3	2000 ℃	Solid-state reactive sintering	[122]
	Silica, alumina, B_2O_3, ZnO, K_2O	1600 ℃	Solid-state reactive sintering	[124]
Electronic component	Aluminum isopropoxide, tetraethyl orthosilicate, 0.5 M solution of aluminum nitrate nonahydrate, metal salts	1000-1300 ℃	Sol-gel	[125]
	Clay, aluminum isopropoxide	1000-1400 ℃	Solid-state reactive sintering	[126]
	Kaolinite clay, mica-rich kaolin waste	1400 ℃	Solid-state reactive sintering	[28]
Matrix and reinforcement of composite material	Bauxite, colloidal silica suspension	1600 ℃	Solid-state reactive sintering	[128]
	Commercial cordierite, clay, talc, andalusite, SiC aggregates	1375 ℃	Solid-state reactive sintering	[131]
	Gibbsite, zirconia, kaolinite, TiO_2, ZnO	1250-1550 ℃	Solid-state reactive sintering	[132]
	Carbon fibers, Al_2O_3 powder, SiO_2 powder, Y_2O_3	1500 ℃	Spark plasma sintering	[133]
	Carbon fibers, Al_2O_3-SiO_2 sol	1300 ℃	Sol-gel	[135]
	Carbon fibers, Al_2O_3-SiO_2 sol	1400 ℃	Sol-gel	[136]
	Carbon fibers, Al_2O_3-SiO_2 sol	1300 ℃	Sol-gel	[137]

[111, 112], porcelains [113, 114], porous high-resistance ceramics [115-119], membranes [18, 120, 121], crucibles [106], optical [122-124] and electronic components [28, 124-127], and matrix and reinforcement of composite materials [18, 128-137]. In recent years, many studies have been carried out to diversify the raw materials and methods used for the synthesis of mullite and, in this way, to further expand its applicability. Table II lists some of these studies.

Refractories: mullite refractories are widely applied to components and accessories of high-temperature furnaces, such as mats, plates, jars, and crucibles, due to the excellent resistance of these materials at high temperatures [109]. Since the late Middle Ages, the crucibles manufactured in the German villages of Epterode and Almerode (current Groβalmerode in the region of Hesse) have been very desired by researchers, chemists, metallurgists, and jewelers due to its exceptional quality, considered by many as a mystery. Martinón-Torres et al. [106] suggested that the main secret behind the superior quality of these crucibles was the development of mullite during manufacture. After analyzing

50 crucibles obtained in the Hesse region, the authors reported that they were made according to a standardized method, using a kaolinitic clay with relatively pure quartz sand and high firing temperatures. Then, the researchers confirmed the presence of the mullite phase in the material, probably crystallized after the decomposition of kaolinite at temperatures above 1300 °C. These crucibles demonstrated high chemical, creep, and thermal shock resistances and high refractoriness, which explains their remarkable success in the international market.

The high cost of raw materials traditionally used in the manufacture of mullite ceramic products has driven the scientific community to find alternative materials and improvements in synthesis, in order to reduce costs. In recent years, several studies [63, 69, 106-108, 115, 127, 138] have been carried out seeking to replace traditional raw materials with low-cost minerals and different types of waste [110]. Chen et al. [110] prepared light mullite-corundum refractory using commercial tabular alumina, reactive alumina, silica, and mullite. The researchers found that the interlocking mullite crystals greatly improved the mechanical strength and thermal shock resistance of the refractory material. Khalil and Algamal [105] prepared mullite refractories using residues from the ceramic industry, rich in aluminosilicates, and bauxite. The feasibility of producing high-performance refractory material with up to 40 wt% of ceramic waste and 60 wt% of crude bauxite has been confirmed. Luo et al. [107] prepared mullite ceramics for coating using only high alumina fly ash and relatively low sintering temperatures (1100-1400 °C). Samples sintered at 1300 °C exhibited mullite crystals and good properties (relative density: 90.85%, water absorption: 0.10%, modulus of rupture: 109.67 MPa, linear shrinkage: 15.70%, and apparent porosity: 0.68%). Lu et al. [108] produced mullite ceramics for coating using coal fly ash and different sources of alumina [$Al(OH)_3$, Al_2O_3, and boehmite]. The researchers found that the optimum sintering temperature was 1100 °C and among the different sources of alumina, boehmite was the one that promoted the greatest densification and crystallization of ceramics.

Porous ceramics: porous mullite-based ceramics have been extensively investigated for many important applications, such as thermal insulation, filtration, and support for catalysts due to their lightness, high melting point, low thermal conductivity, high surface area, and good chemical inertness [116]. These materials have been produced from different types of raw materials rich in SiO_2 and Al_2O_3, from fine chemical compounds, minerals, and residues [115], using different methods and techniques, including the polymeric sponge replication, the addition of pore-forming agents, and gelcasting [116]. Zhu and Yan [115] prepared porous mullite-based ceramics using coal fly ash from a thermoelectric power plant. Al_2O_3, starch, and polyurethane sponges were used, respectively, as an additive, curing agent, and polymeric mold. The researchers identified mullite as the major crystalline phase in all samples and observed its increase according to the increase in the content of Al_2O_3. Han et al. [116] prepared high-strength porous mullite ceramics using a combination of gelcasting and microwave sintering methods. For this, they used pastes containing 52 vol% of powdered mullite, 0.5 wt% of Isobam 104, and 0.1 wt% of carboxymethylcellulose, with 1.0 vol% of triethanolamine lauryl sulfate added to generate foam. Samples sintered at 1373 K showed porosity values (76.6%), thermal conductivity (0.269 W.m^{-1}.K^{-1}), and compressive strength (15.2 MPa) comparable or even better than those presented by porous mullite ceramics sintered by conventional heating at very high temperatures (1573-1873 K). Ma et al. [117] successfully prepared porous mullite ceramics using coal fly ash as a major raw material. Bauxite and V_2O_5 were used, respectively, as a source of Al_2O_3 and sintering agent, while SiC and potassium feldspar were used to improve pore characteristics. Porous mullite ceramics produced with 10 wt% of SiC and 4-12 wt% of potassium feldspar obtained adequate properties. The ranges of closed porosity, compressive strength, and thermal conductivity were 14.79-18.57%, 217.18-236.67 MPa, and 2.19-2.52 W.m^{-1}.K^{-1} (800 °C), respectively. The researchers found that the increase in the SiC content and the elevation of the sintering temperature contributed to the improvement of the compressive strength and thermal shock resistance of the samples.

Membranes: ceramic membranes are widely applied in filtration processes in corrosive, fouling, and high-temperature environments. They have high potential in applications such as sewage treatments, groundwater, and industrial effluents due to their high mechanical resistance, high chemical and thermal stability, good anti-fouling properties, and long useful life when compared to polymeric membranes [18]. According to Twibi et al. [139], mullite can be considered a cost-effective material with high physical properties to fabricate ceramic membranes. The low-cost materials used in producing mullite-based ceramic materials require a lower sintering temperature compared to purified metal oxide-based materials. Mullite can also be used to improve membrane mechanical strength as the calcination process during mullite processing impacts better strength [121, 140, 141]. Rashad et al. [18] developed ceramic membranes of mullite and mullite-alumina using a China clay, $AlF_3.3H_2O$, and different contents of Al_2O_3. It was verified the formation of a network of mullite crystals highly interlaced in the samples with 10 wt% of alumina and sintered at 1400 °C, which contributed to the development of porous samples (apparent porosity of 64%) with good strength (43 MPa) and 889 L.m^{-2}.h^{-1}.bar^{-1} pure water flow. The researchers concluded that the developed ceramic membranes can be used directly in microfiltration processes or as a support for additional membrane layers for separation processes. Fu et al. [120] prepared mullite-based ceramic membranes using coal fly ash and $Al(OH)_3$ as the main raw materials. MoO_3 (0-20 wt%) was used as a sintering additive. The results revealed that MoO_3 effectively inhibited membrane densification and, at the same time, contributed to the formation of a low viscosity metastable liquid at lower temperatures. This allowed the formation of

a more porous structure and the growth of mullite crystals with controllable morphologies. The open porosity of the membranes varied from 42% to 58%, at 1300 ºC, according to the MoO_3 content, without significant degradation in the flexural strength, which was 45 to 36 MPa. Liu et al. [121] developed highly porous mullite ceramic membranes for the microfiltration of emulsified oily wastewater. For this, they used coal gangue, $Al(OH)_3$, and $(NH_4)_6Mo_7O_{24}.4H_2O$ as a source of MoO_3. The researchers found that the use of a MoO_3 source favored the mullitization reactions and contributed to the growth of the mullite crystals that inhibit densification resulting in a high porosity ceramic membrane. The membrane sintered at 1400 ºC showed the most satisfactory results, such as: high open porosity (47.21%), average pore size of 185.3 nm, flexural strength of 34 MPa, permeability of 35.8 $mL.m^{-2}.s^{-1}$, and oil rejection above 97% when operating at 0.1 MPa of transmembrane pressure in oil-water separation experiments. Thus, the authors concluded that the prepared microfiltration membrane is suitable for use in the treatment of oily wastewater.

Optical components: the optical translucency of mullite ceramics, in combination with its excellent thermal shock resistance, makes the application of this material suitable in the manufacture of optical windows for high-temperature environments [122]. Schneider et al. [122] studied the optical transmittance of mullite ceramics in the spectrum bands in the near-infrared (NIR), visible light (VIS), and ultraviolet (UV) regions. To carry out the study, the researchers used powdered mullite of high purity, produced by reactive sintering in the liquid state with minimal amounts of α-Al_2O_3 and glassy phase in the production of the specimens that were manufactured without pressure and by hot isostatic pressing. Both processing methods provided fine-grained microstructures (average grain size of 5-10 μm). The optically translucent mullite hot isostatically pressed presented porosity lower than 1%, a transmittance of 40% in the VIS range, and up to 80% in the NIR range, being considered the most suitable for optical windows in the VIS and NIR ranges, particularly at high temperatures. Golshan et al. [124] prepared transparent mullite glass-ceramics based on the SiO_2-Al_2O_3-B_2O_3-ZnO-K_2O system. The components were thoroughly mixed in a mortar and then melted in an alumina crucible at 1600 °C. The heat treatment of vitreous specimens must be conducted to form the largest amount of mullite possible and at the same time preserve the transparency of the resulting vitreous ceramic. Therefore, the glasses were heat-treated at various temperatures. The results revealed that the best temperature for obtaining mullite glass-ceramics was 850 ºC, which led to the precipitation of 22 wt% of mullite. The authors concluded that mullite crystallized voluminously inside the glass samples, resulting in a transparent glassy ceramic, which showed an intense emission of photoluminescence at 700 nm when excited by a light beam with a wavelength of 590 nm. The doping of rare-earth ions in mullite for the modification of optical devices is currently gaining attention. Islam et al. [141] used the sol-gel method at room temperature to prepare mullite matrices

doped with erbium (Er). According to the researchers, the matrices obtained were considered photoluminescent, thermally stable, transparent, and with a high refractive index, which is very promising for applications in optical devices.

Electronic components: mullite and mullite-based composites that have low dielectric constant and low losses at high frequencies are suitable for several engineering applications, such as packaging for high-frequency circuits, electronic substrates, and ceramic capacitors [125-128]. Roy et al. [125] prepared mullite composites using the sol-gel technique in the presence of transition metal ions. A better crystallization of mullite was verified with the increase of the concentration of metal ions. The dielectric constant of the composites followed a typical trend observed in ceramic materials, that is, it decreased according to the increase in frequency for all samples that reached high-frequency constancy (1.5 Hz). The researchers concluded that the nickel-doped mullite nanocomposites, which presented good high-frequency dielectric properties, are suitable for use on electronic substrates. Kool et al. [126] developed a highly dense mullite-alumina composite using clay aggregates from the Ganges riverbed, in India, and aluminum isopropoxide. The researchers observed the formation of equiaxial and elongated mullite crystals. The mechanical characteristics of the composite were measured in terms of relative density and Vickers hardness, which were approximately 89% and 4.5 GPa at 1400 ºC, respectively. It was verified a dielectric constant of approximately 18 at 1400 ºC, higher than that of alumina or mullite. The authors concluded that the material can be used in structural, electrical, and optical applications. Andrade et al. [28] produced mullite-based composites by reactive sintering in solid-state of kaolinitic clay and mixtures with kaolin residues, rich in mica. The authors observed that a viscous flow resulting from the vitreous phase filled the open porosity and increased the mechanical strength. The electrical conductivity ($1.02x10^{-7}$-$4.49x10^{-7}$ S/cm at 400 ºC), the dielectric constant (6-7.5 at 1 MHz and 30 ºC) and the dielectric loss (0.0004 and 0.001 at 1 MHz and 30 ºC) were strongly dependent on microstructural characteristics (glassy phase and porosity). The activation energies (0.89-0.99 eV) for electrical conduction were low. Therefore, composites synthesized with up to 53.6% of mullite (uniformly dispersed in a glass matrix) can be considered completely suitable for applications related to electronics, in addition to having a low cost.

Matrix and reinforcement of composite materials: manufacturing strong and damage-tolerant composites is a challenge due to the intrinsic brittleness and low fracture toughness of ceramic materials. For this reason, many studies have been developed in order to manufacture mullite matrix composites with favorable properties [130]. Mullite-zirconia, mullite-cordierite, and mullite-corundum composites are widely known for their applications as refractories. High chemical stability, thermal shock resistance, and adequate mechanical properties, specifically high fracture toughness, are some of the characteristics that

make these materials potential candidates for traditional and advanced industries [130-132]. Maldhure et al. [128] prepared mullite-corundum composites using bauxite as the major raw material. The researchers found that the mullite content favors the performance of the material in terms of mechanical strength at high temperatures, thermal shock resistance, and crack propagation. Kakroudi et al. [131] produced mullite-cordierite composites so that mullite particles were formed *in situ*, from the mixture of andalusite, talc, alumina, and 15 wt% of SiC. It was observed the dependence between the content of SiC and the thermal shock resistance and modulus of elasticity. The addition of 5 wt% of SiC was considered the ideal amount to obtain the best performance of the mullite-cordierite composite. Sistani et al. [132] investigated the microstructural properties, mechanical strength, and surface roughness of zirconia-mullite composites. The simultaneous effect of the duration of the mechanical activation process by grinding and the addition of TiO_2 and ZnO were studied. The researchers observed mullite as the major crystalline phase in samples containing TiO_2 that were mechanically activated for 6-24 h and sintered at 1450 ºC, and in mechanically activated for 6-72 h and sintered at 1550 ºC. In the compositions with ZnO, submitted to mechanical activation for 6-72 h, the effective crystallization of mullite was verified only at 1550 ºC. The prolongation of the mechanical activation process, from 6 to 72 h, promoted the elimination of the acicular morphology of the mullite phase, in addition to notably increasing the Weibull modulus and decreasing the apparent roughness values because of greater homogeneity.

Mullite-carbon composites are considered promising candidates to be applied in high-temperature electromagnetic interference (EMI) shielding devices in the gigahertz band. Electrical conductivity and dielectric permittivity are widely recognized as key factors in determining protection against electromagnetic interference in these composites [133]. Ru et al. [134] reported that the excellent conductivity of the graphene-mullite composite, coupled with its high mechanical strength, provides a high-performance EMI shield. Xia et al. [133] found excellent electromagnetic properties and a high EMI shielding effectiveness value (~40 dB) for carbon-mullite composites with 1.65 vol% of carbon and 2 mm thickness. Mullite matrix composites reinforced with pre-molded 3D carbon fibers have attracted the interest of the scientific community, as it is an alternative to overcome the inherent fragility of monolithic mullite ceramics [134]. Zhang et al. [136, 137] observed satisfactory mechanical properties in mullite composites, prepared from sol of Al_2O_3-SiO_2 with a high content of solids, and reinforced with pre-molded 3D carbon fibers. To further optimize the performance of these composites, Zhang et al. [137] introduced a PyC-SiC double-layer interfacial coating. The researchers noted that the coating played a positive role in protecting the carbon fiber, weakening the interfacial bond, and alleviating the thermal incompatibility between the fiber and the matrix. Consequently, mechanical strength and thermal shock resistance have been improved.

FINAL REMARKS

There are many reviews about mullite in literature, but not so many that provide such a complete set of up-to-date information associated with the microstructural characteristics, properties, preparation methods, and applications. As shown in this review, mullite has properties (such as high thermal stability and excellent thermal shock resistance, low thermal expansion and conductivity, good mechanical strength, and creep resistance) that give it great technological importance and numerous application possibilities in the most diverse fields of engineering. Therefore, due to the great importance of this material, it is necessary to constantly search for alternative raw materials that can be used in its manufacture, new approaches regarding synthesis methodologies, and more knowledge about how the synthesis variables can affect the final microstructure. In addition, in-depth knowledge of these materials is of great importance, so that it is possible to overcome challenges such as the densification of mullite at low temperatures and improvement in its fracture toughness.

ACKNOWLEDGMENT

REFERENCES

[1] R.H. Doremus, J.F. Shackelford (Eds.), "Ceramic and glass materials: structure, properties and processing", Springer, Boston (2008).

[2] H. Schneider, J. Schreuer, B. Hildmann, J. Eur. Ceram. Soc. **28** (2008) 329.

[3] D. Ibrahim, S. Naga, Z.A. Kader, E.A. Salam, Ceram. Int. **21** (1995) 265.

[4] R.R. Menezes, F.F. Farias, M.F. Oliveira, L.N. Santana, G.A. Neves, H.L. Lira, H.C. Ferreira, Waste Manag. Res. **27** (2009) 78.

[5] M. Hosseinzadeh, M. Akbari, F. Bashiri, in "30th Int. Power Syst. Conf." (2015) 371.

[6] P. Rodrigo, P. Boch, Int. J. Appl. Ceram. Technol. **1** (1985) 3.

[7] Y. Dong, B. Lin, S. Wang, K. Xie, D. Fang, X. Zhang, H. Ding, X. Liu, G. Meng, J. Alloys Compd. **477** (2009) L35.

[8] J. Ma, F. Ye, B. Zhang, Y. Jin, C. Yang, J. Ding, H. Zhang, Q. Liu, Ceram. Int. **44** (2018) 13320.

[9] P. Sánchez-Soto, D. Eliche-Quesada, S. Martínez-Martínez, E. Garzón-Garzón, L. Pérez-Villarejo, J.M. Rincón, Mater. Lett. **223** (2018) 154.

[10] H. Schneider, S. Komarneni, *Mullite*, Wiley-VCH, Weinheim (2005).

[11] Oschatz, Wächter (1847), in: K. Litzow, *Keramische technik: von irdengut zum porzellan*, Callway, Munich (1984).

[12] S.C. Deville, D. Caron (1865), in: J.A. Pask, "Mullite

and mullite matrix composites", Ceram. Trans. **6** (1990) 1.

[13] W.I. Vernadsky (1890), in: J.A. Pask, "Mullite and mullite matrix composites", Ceram. Trans. **6** (1990) 1.

[14] N. Bowen, J. Greig, J. Am. Ceram. Soc. **7** (1924) 238.

[15] H. Schneider, R.X. Fischer, J. Schreuer, D.J. Green, J. Am. Ceram. Soc. **98** (2015) 2948.

[16] Web of Science, "Mullite records", clarivate.com/webofsciencegroup, ac. Aug. 20, 2021.

[17] H. Tan, Y. Ding, J. Yang, J. Alloys Compd. **492** (2010) 396.

[18] M. Rashad, U. Sabu, G. Logesh, M. Balasubramanian, Sep. Purif. Technol. **219** (2019) 74.

[19] L. Zhang, G.-C. Han, IOP Conf. Ser. Earth Environ. Sci. **267** (2019) 22045.

[20] B.R. Johnson, W.M. Kriven, J. Schneider, J. Eur. Ceram. Soc. **21** (2001) 2541.

[21] J. Anggono, J. Tekn. Mesin **7** (2005) 1.

[22] R. Farias, R. Menezes, E. Medeiros, J. Oliveira, Rev. Eletr. Mater. Process. **10** (2015) 1.

[23] T.F. Krenzel, J. Schreuer, D. Laubner, M. Cichocki, H. Schneider, J. Am. Ceram. Soc. **102** (2019) 416.

[24] M. Schmücker, H. Schneider, K.J. MacKenzie, M.E. Smith, D.L. Carroll, J. Am. Ceram. Soc. **88** (2005) 2935.

[25] C.B. Carter, M.G. Norton, *Ceramic materials: science and engineering*, Springer, New York (2013).

[26] J. Holm, J. Mater. Sci. Lett. **21** (2002) 1551.

[27] W. Lee, G. Souza, C. McConville, T. Tarvornpanich, Y. Iqbal, J. Eur. Ceram. Soc. **28** (2008) 465.

[28] R.M. Andrade, A.J. Araújo, H.P. Alves, J.P. Grilo, R.P. Dutra, L.F. Campos, D.A. Macedo, Ceram. Int. **45** (2019) 18509.

[29] R.R. Menezes, P.M. Souto, R.H.G.A. Kiminami, Cerâmica **53**, 327 (2007) 218.

[30] P.M. Souto, R.R. Menezes, R.H.G.A. Kiminami, Cerâmica **57**, 344 (2011) 438.

[31] H. Mao, M. Selleby, B. Sundman, J. Am. Ceram. Soc. **88** (2005) 2544.

[32] I. Aksay, J. Pask, J. Am. Ceram. Soc. **58** (1975) 507.

[33] S. Chaudhuri, Ceram. Int. **13** (1987) 167.

[34] N.A. Toropov, F.Y. Galakhov, Dokl. Akad. Nauk SSSR **78** (1951) 299.

[35] A. Staronka, H. Pham, M. Rolin, Rev. Int. Hautes Temp. **5** (1968) 111.

[36] S. Aramaki, R. Roy, J. Am. Ceram. Soc. **45** (1962) 229.

[37] F.J. Klug, S. Prochazka, R.H. Doremus, J. Am. Ceram. Soc. **70** (1987) 750.

[38] G. Gelsdorf, H. Müller Hesse, H.E. Schwiete, Arch. Eisenhüttenw. **29** (1958) 513.

[39] V. Skola, Keram. Rundsch. Kunst. Keram. **45** (1937) 188.

[40] S.H. Risbud, J.A. Pask, J. Mater. Sci. **13** (1978) 2449.

[41] G. Tromel, K.H. Obst, K. Konopicky, H. Bauer, I. Patzak, Ber. Deut. Keram. Ges. **34** (1957) 397.

[42] S. Chaudhuri, Ceram. Int. **13** (1987) 177.

[43] R. Liu, J. Yuan, C.-A. Wang, J. Eur. Ceram. Soc. **33** (2013) 3249.

[44] J. Cao, X. Dong, L. Li, Y. Dong, S. Hampshire, J. Eur.

Ceram. Soc. **34** (2014) 3181.

[45] E. Bartonickova, P. Ptacek, T. Opravil, F. Soukal, J. Masilko, R. Novotny, J. Svec, J. Havlica, Ceram. Int. **41** (2015) 14116.

[46] D.L. da Silva, A.V. da Silva, H.S. Ferreira, Cerâmica **62**, 363 (2016) 294.

[47] M. Yan, Y. Li, Y. Sun, L. Li, S. Tong, J. Sun, Mater. Chem. Phys. **202** (2017) 245.

[48] T.I. Mah, K. Mazdiyasni, J. Am. Ceram. Soc. **66** (1983) 699.

[49] M. Osendi, C. Baudin, J. Eur. Ceram. Soc. **16** (1996) 217.

[50] S. Kanzaki, H. Tabata, T. Kumazawa, Ceram. Trans. **6** (1990) 339.

[51] M. Mizuno, J. Am. Ceram. Soc. **74** (1991) 3017.

[52] M. Malki, J. Schreuer, H. Schneider, Am. Mineral. **99** (2014) 1104.

[53] A. Braga, J. Duarte-Neto, R. Menezes, H. Lira, G. Neves, Rev. Eletr. Mater. Process. **9** (2014) 60.

[54] H. Guo, F. Ye, W. Li, X. Song, G. Xie, Ceram. Int. **41** (2015) 14645.

[55] H. Guo, W. Li, F. Ye, Ceram. Int. **42** (2016) 4819.

[56] H. Guo, W. Li, J. Eur. Ceram. Soc. **38** (2018) 679.

[57] B. Li, M. He, H. Wang, Metall. Mater. Trans. A Phys. Metall. Mater. Sci. **48** (2017) 3188.

[58] X. Xu, J. Li, J. Wu, Z. Tang, L. Chen, Y. Li, C. Lu, Ceram. Int. **43** (2017) 1762.

[59] M. Bouchetou, J. Poirier, L.A. Morales, T. Chotard, O. Joubert, M. Weissenbacher, Ceram. Int. **45** (2019) 12832.

[60] M.V.M. Magliano, V.C. Pandolfelli, Cerâmica **56**, 340 (2010) 368.

[61] J. Bai, Ceram. Int. **36** (2010) 673.

[62] K. Okada, J. Eur. Ceram. Soc. **28** (2008) 377.

[63] V.J. da Silva, M.F. da Silva, W.P. Gonçalves, R.R. de Menezes, G.D. Araújo Neves, H.D. Lucena Lira, L.N. de Lima Santana, Ceram. Int. **42** (2016) 15471.

[64] H. Yahya, M.R. Othman, Z.A. Ahmad, Procedia Chem. **19** (2016) 922.

[65] T. Sahraoui, H. Belhouchet, M. Heraiz, N. Brihi, A. Guermat, Ceram. Int. **42** (2016) 12185.

[66] L. Kong, Y. Gan, J. Ma, T. Zhang, F. Boey, R. Zhang, J. Alloys Compd. **351** (2003) 264.

[67] H. Aripin, S. Mitsudo, E. Prima, I. Sudiana, H. Kikuchi, S. Sano, S. Sabchevski, Ceram. Int. **41** (2015) 6488.

[68] L. Chen, Z. Wang, S. Hu, X. Qin, Z. Xue, G. Zhou, S. Wang, Ceram. Int. **47** (2021) 13762.

[69] W. Zhou, W. Yan, N. Li, Y. Li, Y. Dai, B. Han, Y. Wei, Ceram. Int. **44** (2018) 22950.

[70] H.-J. Kleebe, F. Siegelin, T. Straubinger, G. Ziegler, J. Eur. Ceram. Soc. **21** (2001) 2521.

[71] W.P. Gonçalves, V.J. Silva, R.R. Menezes, G.A. Neves, H.L. Lira, L.N.L. Santana, Appl. Clay Sci. **137** (2017) 259.

[72] L.L. Sousa, A.D.V. Souza, L. Fernandes, V.L. Arantes, R. Salomão, Ceram. Int. **41** (2015) 9443.

[73] S. Li, H. Du, A. Guo, H. Xu, D. Yang, Ceram. Int. **38** (2012) 1027.

[74] K. Okada, N. Otuska, J. Am. Ceram. Soc. **74** (1991)

2414.

[75] X. Ji, F. Xu, H. Chen, Adv. Mater. Res. **79-82** (2009) 1983.

[76] S.M. Naga, A. El-Maghraby, Mater. Charact. **62** (2011) 174.

[77] G. Chen, H. Qi, W. Xing, N. Xu, J. Membr. Sci. **318** (2008) 38.

[78] J. Cao, X. Dong, L. Li, Y. Dong, S. Hampshire, J. Eur. Ceram. Soc. **34** (2014) 3181.

[79] R.M. Khattab, A.M. El-Rafei, M.F. Zawrah, Mater. Res. Bull. **47** (2012) 2662.

[80] B. Sandberg, T. Mosberg, Ceram. Trans. **4** (1989) 245.

[81] R. Salomão, V.C. Pandolfelli, Am. Ceram. Soc. Bull. **86** (2007) 9301.

[82] R.F. Davis, J.A. Pask, J. Am. Ceram. Soc. **55** (1972) 525.

[83] J.A. Pask, Ceram. Int. **9** (1983) 107.

[84] F. Kara, J.A. Little, J. Eur. Ceram. Soc. **16** (1996) 627.

[85] W.G. Farenholtz, D.M. Smith, J. Cesarano III, J. Am. Ceram. Soc. **76** (1993) 433.

[86] B. Saruban, W. Albers, H. Schneider, W.A. Kaysser, J. Eur. Ceram. Soc. **16** (1996) 1075.

[87] S. Kanzani, H. Tabata, T. Kumazawa, S. Ohta, J. Am. Ceram. Soc. **68** (1985) C6.

[88] D.A. Rani, D.D. Jayaseelan, F.D. Gnanam, J. Eur. Ceram. Soc. **21** (2001) 2253.

[89] F. Yang, C. Lin, Y. Li, C.A. Wang, Mater. Lett. **73** (2012) 36.

[90] H. Schneider, U. Seifert-Kraus, A. Majdic, Am. Ceram. Soc. Bull. **61** (1982) 741.

[91] Z.Y. Deng, T. Fukasawa, M. Ando, J. Am. Ceram. Soc. **84** (2001) 485.

[92] A.D.V. Souza, C.C. Arruda, L. Fernandez, M.L.P. Antunes, P.K. Kiyohara, R. Salomão, J. Eur. Ceram. Soc. **35** (2015) 803.

[93] L. Fernandes, C.C. Arruda, A.D.V. Souza, R. Salomão, Int. Ceram. Rev. **63** (2014) 220.

[94] J.A. Pask, J. Eur. Ceram. Soc. **16** (1996) 101.

[95] S.K.S. Hossain, R. Pyare, P.K. Roy, Ceram. Int. **46** (2020) 10871.

[96] M. Srivastava, M. Muniprakash, S. Singh, Surf. Coat. Technol. **245** (2014) 148.

[97] V.V. Kumar, S.S. Kumaran, S. Dhanalakshmi, R. Sivaramakrishnan, J. Braz. Soc. Mech. Sci. Eng. **41** (2019) 179.

[98] L.S. Cividanes, T.M. Campos, L.A. Rodrigues, D.D. Brunelli, G.P. Thim, J. Sol-Gel Sci. Technol. **55** (2010) 111.

[99] S. Chaudhuri, S. Patra, Br. Ceram. Trans. **96** (1997) 105.

[100] G. Feng, F. Jiang, W. Jiang, J. Liu, Q. Zhang, Q. Wu, Q. Hu, L. Miao, Ceram. Int. **44** (2018) 22904.

[101] R.S. Hiratsuka, C.V. Santilli, S.H. Pulcinelli, Quím. Nova **18** (1995) 171.

[102] H. Schneider, K. Okada, J.A. Pask, S. Rahman, *Mullite and mullite ceramics*, J. Wiley, New York (1994).

[103] S. Sundaresan, I.A. Aksay, J. Am. Ceram. Soc. **74** (1991) 2388.

[104] H. Rezaie, W. Rainforth, W. Lee, British Ceram. Trans. **96** (1997) 181.

[105] N. Khalil, Y. Algamal, Silicon **12** (2020) 1557.

[106] M. Martinón-Torres, I.C. Freestone, A. Hunt, T. Rehren, J. Am. Ceram. Soc. **91** (2008) 2071.

[107] Y. Luo, S. Ma, S. Zheng, C. Liu, D. Han, X. Wang, J. Alloys Compd. **732** (2018) 828.

[108] J. Lu, Z. Zhang, Y. Li, Z. Liu, Constr. Build. Mater. **229** (2019) 116851.

[109] C. Sadik, I.-E.E. Amrani, A. Albizane, J. Asian Ceram. Soc. **2** (2014) 310.

[110] Y. Chen, G. Liu, Q. Gu, S. Li, B. Fan, R. Zhang, H. Li, Materialia **8** (2019) 100517.

[111] Z.B. Ozturk, J. Ceram. Process. Res. **17** (2016) 555.

[112] K.R. Silva, L.F.A. Campos, L.N.L. Santana, Mater. Res. **22** (2019) 1.

[113] A. Sanz, J. Bastida, A. Caballero, M. Kojdecki, Clay Miner. **53** (2018) 471.

[114] A. Akkus, T. Boyraz, J. Ceram. Process. Res. **20** (2019) 54.

[115] J. Zhu, H. Yan, Ceram. Int. **43** (2017) 12996.

[116] L. Han, X. Deng, F. Li, L. Huang, Y. Pei, L. Dong, S. Li, Q. Jia, H. Zhang, S. Zhang, Ceram. Int. **44** (2018) 14728.

[117] B. Ma, C. Su, X. Ren, Z. Gao, F. Qian, W. Yang, G. Liu, H. Li, J. Yu, Q. Zhu, J. Alloys Compd. **803** (2019) 981.

[118] R. Liu, X. Dong, S. Xie, T. Jia, Y. Xue, J. Liu, W. Jing, A. Guo, Chem. Eng. J. **360** (2019) 464.

[119] Y. Zhang, Y. Wu, X. Yang, D. Li, X. Zhang, X. Dong, X. Yao, J. Liu, A. Guo, J. Eur. Ceram. Soc. **40** (2020) 2090.

[120] M. Fu, J. Liu, X. Dong, L. Zhu, Y. Dong, S. Hampshire, J. Eur. Ceram. Soc. **39** (2019) 5320.

[121] M. Liu, Z. Zhu, Z. Zhang, Y. Chu, B. Yuan, Z. Wei, Sep. Purif. Technol. **237** (2020) 116483.

[122] H. Schneider, M. Schmücker, K. Ikeda, W.A. Kaysser, J. Am. Ceram. Soc. **76** (1993) 2912.

[123] M. Sales, C. Valentin, J. Alarcón, J. Sol-Gel Sci. Technol. **8** (1997) 871.

[124] N.H. Golshan, B.E. Yekta, V. Marghussian, Opt. Mater. **34** (2012) 596.

[125] D. Roy, B. Bagchi, S. Das, P. Nandy, Mater. Chem. Phys. **138** (2013) 375.

[126] A. Kool, P. Thakur, B. Bagchi, N.A. Hoque, S. Das, Appl. Clay Sci. **114** (2015) 349.

[127] V.J. da Silva, E.P. de Almeida, W.P. Gonçalves, R.B. da Nóbrega, G.A. Neves, H.L. Lira, R.R. Menezes, L.N.L. Santana, Ceram. Int. **45** (2019) 4692.

[128] A.V. Maldhure, H.S. Tripathi, A. Ghosh, Int. J. Appl. Ceram. Technol. **12** (2015) 860.

[129] D. Liu, P. Hu, C. Fang, W. Han, Ceram. Int. **44** (2018) 13487.

[130] D. Liu, M. Tan, C. Fang, W. Han, Ceram. Int. **45** (2019) 304.

[131] M.G. Kakroudi, N.P. Vafa, M.S. Asl, M. Shokouhimehr, Ceram. Int. **46** (2020) 23780.

[132] P.B. Sistani, S.M. Beidokhti, A. Kiani-Rashid, Ceram. Int. **46** (2020) 1472.

[133] X. Xia, Y. Li, L. Long, P. Xiao, H. Luo, L. Pang, X.

Xiao, W. Zhou, J. Eur. Ceram. Soc. **40** (2020) 3423.

[134] J. Ru, Y. Fan, W. Zhou, Z. Zhou, T. Wang, R. Liu, J. Yang, X. Lu, J. Wang, C. Ji, ACS Appl. Mater. Interfaces **10** (2018) 39245.

[135] W. Zhang, Q. Ma, K. Zeng, W. Mao, Ceram. Int. **46** (2020) 9924.

[136] W. Zhang, K.-W. Dai, W.-G. Mao, Trans. Nonferrous Met. Soc. China **28** (2018) 2248.

[137] W. Zhang, Q. Ma, K. Zeng, S. Liang, W. Mao, J. Adv. Ceram. **8** (2019) 218.

[138] Q. Lu, X. Dong, Z. Zhu, Y. Dong, J. Hazard. Mater. **273** (2014) 136.

[139] M.F. Twibi, M.H.D. Othman, S.K. Hubadillah, S.A. Alftessi, T.A. Kurniawan, A.F. Ismail, M.A. Rahman, J. Jaafar, Y.O. Raji, Ceram. Int. **47** (2021) 15367.

[140] R.K. Nishihora, E. Rudolph, M.G.N. Quadri, D. Hotza, K. Rezwan, M. Wilhelm, J. Membr. Sci. **581** (2019) 421.

[141] S. Islam, N. Bidin, S. Riaz, S. Naseem, M.M. Sanagi, J. Taiwan Inst. Chem. Eng. **70** (2017) 366.